Cell Reports, Volume *42*

Supplemental information

The *miR-23-27-24* clusters drive lipid-associated macrophage proliferation in obese adipose tissue

Neil T. Sprenkle, Nathan C. Winn, Kaitlyn E. Bunn, Yang Zhao, Deborah J. Park, Brenna G. Giese, John J. Karijolich, K. Mark Ansel, C. Henrique Serezani, Alyssa H. Hasty, and Heather H. Pua

Figure S1

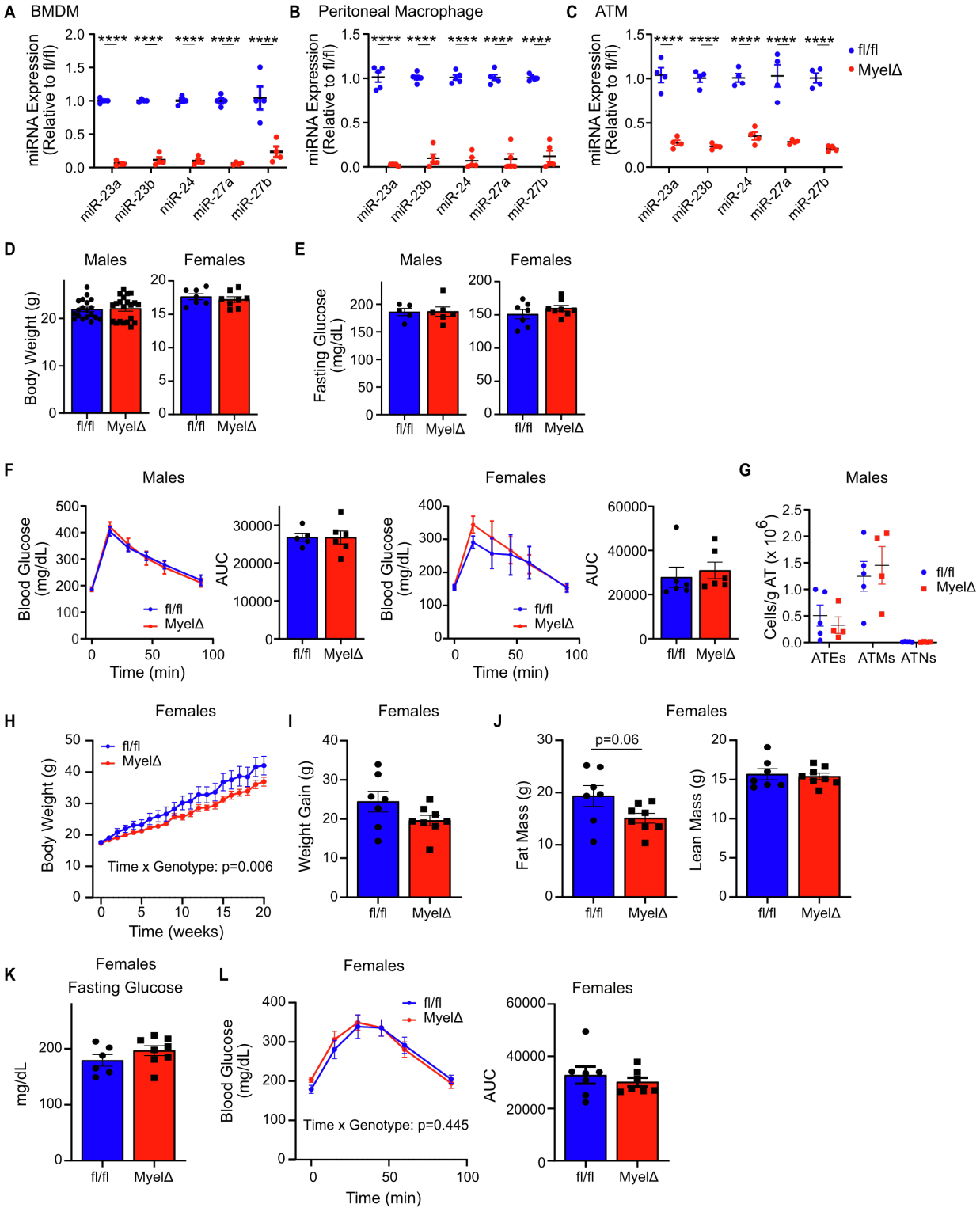
A
BMDM
B
Peritoneal Macrophage
C
ATM
miRNA Expression (Relative to fl/fl)
****
miR-23a
miR-23b
miR-24
miR-27a
miR-27b
fl/fl
MyelΔ
D
Males
Females
Body Weight (g)
E
Fasting Glucose (mg/dL)
F
Blood Glucose (mg/dL)
Time (min)
AUC
G
Cells/g AT (x 10^6)
ATEs
ATMs
ATNs
H
Body Weight (g)
Time x Genotype: p=0.006
Time (weeks)
I
Weight Gain (g)
J
p=0.06
Fat Mass (g)
Lean Mass (g)
K
Fasting Glucose
mg/dL
L
Time x Genotype: p=0.445

Figure S1. Myeloid-Specific Deletion of the *miR-23-27-24* Clusters Does Not Alter Systemic Glucose Tolerance in Male and Female Lean Mice and Obese Female Mice, Related to Figure 1. Relative levels of the indicated miRNAs in (**A**) bone marrow-derived macrophages, (**B**) peritoneal macrophages from lean fl/fl or MyelΔ mice, or (**C**) F4/80-selected ATMs from obese fl/fl or MyelΔ mice (two-way ANOVA with Sidák's multiple comparison test). (**D**) Total bodyweight or (**E**) fasting glucose levels were recorded in lean male or female fl/fl or MyelΔ mice (two-tailed t-test). (**F**) Intraperitoneal glucose tolerance test was performed on lean male or female fl/fl or MyelΔ mice 1 wk before HFD feeding (two-way ANOVA for curves; two-tailed t-test for AUC). (**G**) Myeloid cell numbers were quantified in the epididymal WAT of lean fl/fl or MyelΔ mice (one-way ANOVA with Sidák's multiple comparison test). Female fl/fl or MyelΔ mice were fed a HFD for 20 weeks followed by measurement of (**H**) body weight curves (two-way ANOVA with Sidák's multiple comparison test), (**I**) weight gain (two-tailed t-test), and (**J**) body composition measurements by NMR (two-tailed t-test). (**K**) Fasting glucose levels were recorded following HFD feeding (two-tailed t-test). (**L**) Intraperitoneal glucose tolerance tests (1g/kg lean mass) were performed on female fl/fl and MyelΔ mice following dietary intervention (two-way ANOVA with Sidák's multiple comparison test for curves; two-tailed t-test for area under curve AUC comparisons). Each dot in bar graphs represents one mouse. (**D**-**G**) All lean mice were 7-9 weeks old. (**H**-**L**) Female mice were 8-10 weeks old at beginning of dietary intervention. **H**: 7-8 mice per genotype. ± S.E.M. ****$p<0.0001$.

Figure S2

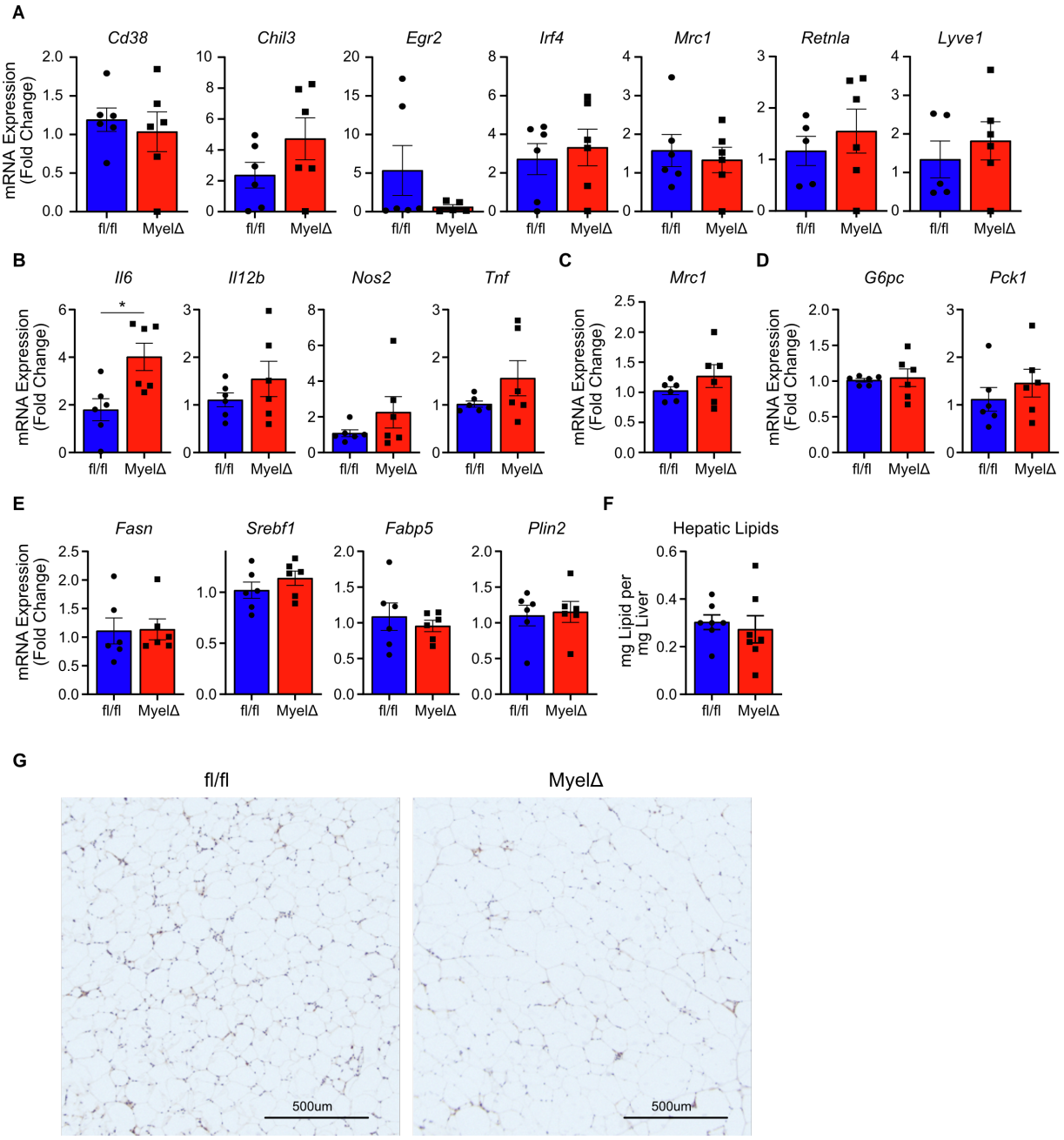

Figure S2. Deficiency of the *miR-23-27-24* Clusters Does Not Reduce mRNA Levels of M2-like Macrophage-Associated Genes in Obese eWAT or Induce Marked Hepatic Dysfunction, Related to Figure 2. (**A**) Levels of M2-like macrophage-associated genes were quantified from eWAT via RT-qPCR (two-tailed t-test). Hepatic mRNA levels of (**B**) pro-inflammatory factors, (**C**) *Mrc1*/CD206, (**D**) gluconeogenic enzymes, or (**E**) lipid metabolism enzymes were compared between obese fl/fl or MyelΔ mice (two-tailed t-test). (**F**) Neutral lipid content was quantified from hepatic tissue from obese fl/fl or MyelΔ mice (two-tailed t-test). (**G**) Representative low-magnification image of epididymal WAT (eWAT) sections stained with anti-F4/80 to visualize crown-like structures. Each dot represents one male mouse after HFD feeding. ± S.E.M. *p≤0.05.

Figure S3

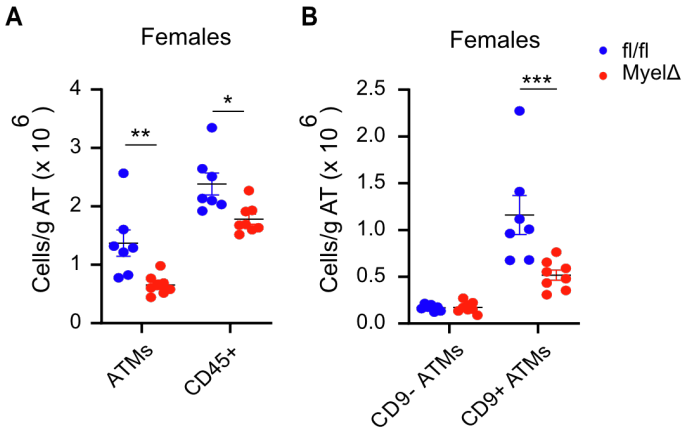

Figure S3. Myeloid-Specific Deletion of the *miR-23-27-24* Clusters Reduces LAM Accrual in Visceral WAT of Female Mice, Related to Figure 2. (**A**) Total ATMs and CD45^{+} immune cells and (**B**) CD9^{-} and CD9^{+} ATMs were quantified from fl/fl and MyelΔ perigonadal WAT of female mice (two-way ANOVA with Sidák's multiple comparison test). Each dot represents one female mouse after HFD feeding. ± S.E.M. *p≤0.05, **p<0.01, ***p<0.001.

Figure S4

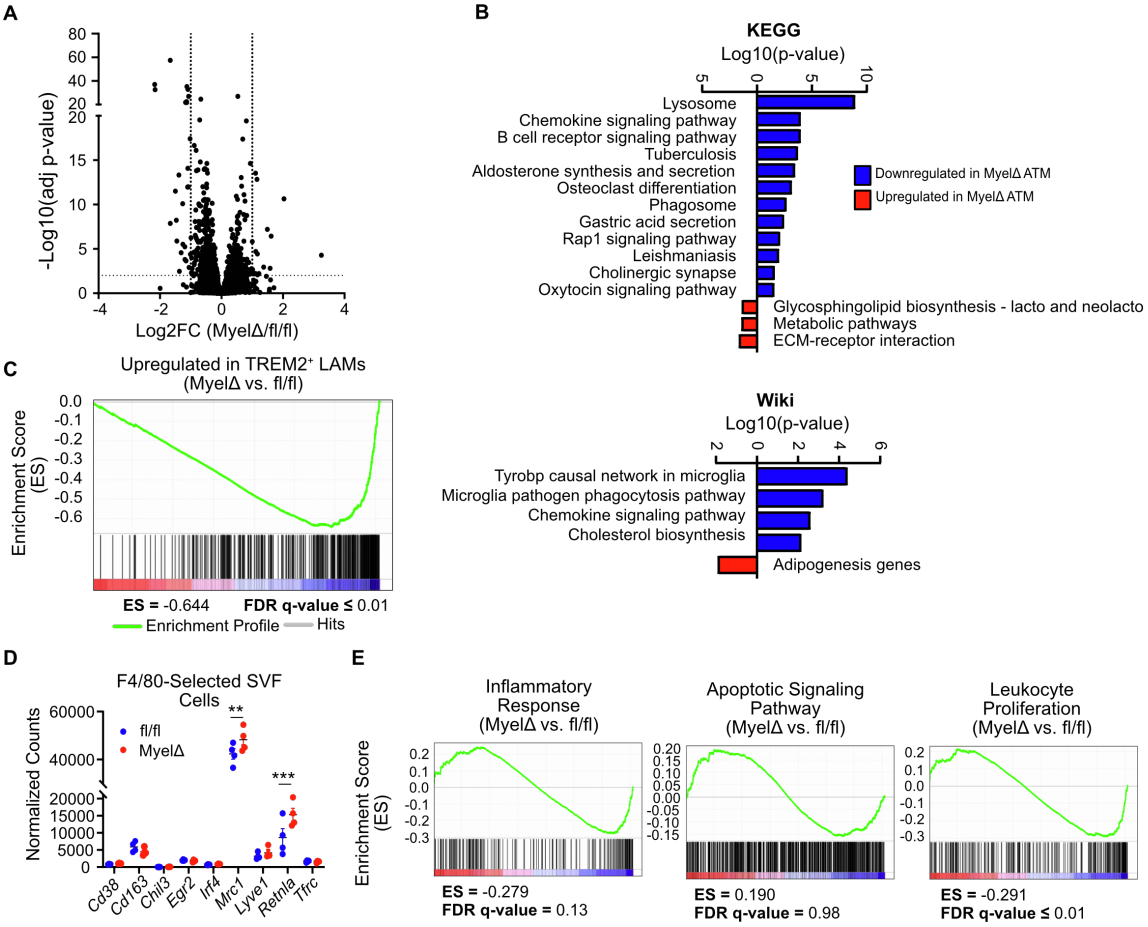

Figure S4. Myeloid-Specific Deletion of the *miR-23-27-24* Clusters Attenuates Expression of Genes Associated with TREM2$^+$ LAMs and Proliferation in Obese ATMs, Related to Figure 4. (**A**) Volcano plot representing transcriptomic changes between F4/80-selected cells from the stromal vascular fraction of obese fl/fl and MyelΔ eWAT (basemean > 100). (**B**) KEGG and Wiki pathway analysis of RNA sequencing (RNA-seq) data. (**C**) Gene set enrichment analysis (GSEA) of RNA-seq data set for genes upregulated in LAMs compared to lean ATMs. (**D**) DESeq2 normalized counts of indicated M2-like macrophage genes were quantified (two-way ANOVA with Sidák's multiple comparison test) (**E**) GSEA of RNA-seq data sets for inflammation, proliferation, and apoptosis. GSEA were plotted with the enrichment curve and rank order location of each gene in the indicated gene set from most upregulated to most downregulated (left to right) in knockout MyelΔ ATMs compared to fl/fl ATMs. Each dot represents one male mouse after HFD feeding. ±S.E.M. **p<0.01, ***p<0.001.

Figure S5

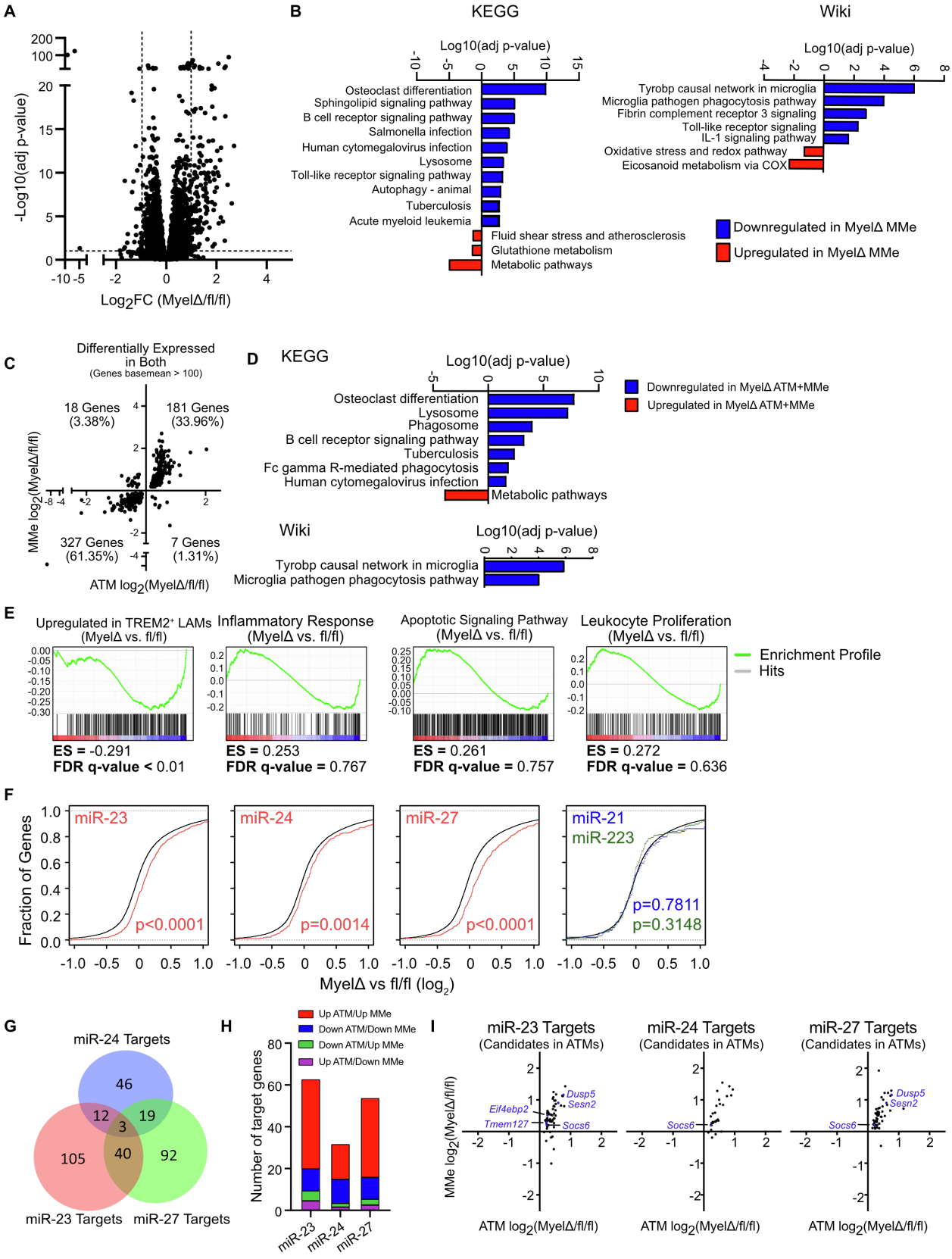
A
-Log10(adj p-value)
Log2FC (MyelΔ/fl/fl)
B
KEGG
Log10(adj p-value)
Osteoclast differentiation
Sphingolipid signaling pathway
B cell receptor signaling pathway
Salmonella infection
Human cytomegalovirus infection
Lysosome
Toll-like receptor signaling pathway
Autophagy - animal
Tuberculosis
Acute myeloid leukemia
Fluid shear stress and atherosclerosis
Glutathione metabolism
Metabolic pathways
Wiki
Log10(adj p-value)
Tyrobp causal network in microglia
Microglia pathogen phagocytosis pathway
Fibrin complement receptor 3 signaling
Toll-like receptor signaling
IL-1 signaling pathway
Oxidative stress and redox pathway
Eicosanoid metabolism via COX
Downregulated in MyelΔ MMe
Upregulated in MyelΔ MMe
C
Differentially Expressed in Both
(Genes basemean > 100)
18 Genes (3.38%)
181 Genes (33.96%)
327 Genes (61.35%)
7 Genes (1.31%)
MMe log2(MyelΔ/fl/fl)
ATM log2(MyelΔ/fl/fl)
D
KEGG
Log10(adj p-value)
Osteoclast differentiation
Lysosome
Phagosome
B cell receptor signaling pathway
Tuberculosis
Fc gamma R-mediated phagocytosis
Human cytomegalovirus infection
Metabolic pathways
Downregulated in MyelΔ ATM+MMe
Upregulated in MyelΔ ATM+MMe
Wiki
Log10(adj p-value)
Tyrobp causal network in microglia
Microglia pathogen phagocytosis pathway
E
Upregulated in TREM2+ LAMs (MyelΔ vs. fl/fl)
ES = -0.291
FDR q-value < 0.01
Inflammatory Response (MyelΔ vs. fl/fl)
ES = 0.253
FDR q-value = 0.767
Apoptotic Signaling Pathway (MyelΔ vs. fl/fl)
ES = 0.261
FDR q-value = 0.757
Leukocyte Proliferation (MyelΔ vs. fl/fl)
ES = 0.272
FDR q-value = 0.636
Enrichment Profile
Hits
F
Fraction of Genes
miR-23
p<0.0001
miR-24
p=0.0014
miR-27
p<0.0001
miR-21
miR-223
p=0.7811
p=0.3148
MyelΔ vs fl/fl (log2)
G
miR-24 Targets
46
12
19
3
105
40
92
miR-23 Targets
miR-27 Targets
H
Up ATM/Up MMe
Down ATM/Down MMe
Down ATM/Up MMe
Up ATM/Down MMe
Number of target genes
miR-23
miR-24
miR-27
I
miR-23 Targets (Candidates in ATMs)
miR-24 Targets (Candidates in ATMs)
miR-27 Targets (Candidates in ATMs)
MMe log2(MyelΔ/fl/fl)
Dusp5
Sesn2
Eif4ebp2
Tmem127
Socs6
ATM log2(MyelΔ/fl/fl)

Figure S5. The *miR-23-27-24* Clusters Transcriptionally Regulate Shared Pathways and Predicted Targets in Metabolically Activated Macrophages and Obese ATMs, Related to Figure 4. (**A**) Volcano plot representing transcriptomic changes between fl/fl and MyelΔ metabolically activated (MMe) BMDMs (basemean > 100). (**B**) KEGG and Wiki pathway analysis of RNA sequencing (RNA-seq) data. (**C**) Log_2(MyelΔ/fl/fl) of differentially expressed genes in both F4/80-selected ATMs and MMe BMDMs were plotted (basemean>100; adjp value≤0.05). (**D**) KEGG and Wiki pathway analysis of genes significantly upregulated or downregulated in both MyelΔ ATMs and MMe BMDMs. (**E**) Gene set enrichment analysis (GSEA) of RNA-seq data from MMe BMDMs for genes upregulated in LAMs compared to lean ATMs or involved in inflammation, apoptosis, or leukocyte proliferation. GSEA were plotted with the enrichment curve and rank order location of each gene in the indicated gene set from most upregulated to most downregulated (left to right) in knockout MyelΔ MMe BMDMs compared to fl/fl MMe BMDMs. (**F**) Cumulative distribution frequency plots depicting global mRNA expression by RNA-seq as log_2(MyelΔ/fl/fl) in MMe BMDMs plotted against the cumulative fraction of all genes (black), miR-23/24/or/27 8mer targets (red), miR-21 targets (blue), or miR-223 targets (green) (Kolmogorov-Smirnov test). Target predictions were made using TargetScan. (**G**) Venn diagram depicting number of shared or unique candidate target genes significantly upregulated in MMe BMDMs whose 3'untranslated region (3'UTR) is predicted to be regulated by miR-23, miR-24, and/or miR-27 (basemean>100; adjp value≤0.05). (**H**) Bar graph indicating distribution of shared candidate target genes among differentially expressed in both obese ATMs and MMe BMDMs (basemean>100; adjp value≤0.05). (**I**) Log_2(MyelΔ/fl/fl) of MMe BMDM and obese ATM of predicted target genes from the indicated miRNA significantly upregulated in obese ATMs. Blue dots represent candidate target genes predicted to regulate proliferation in ATMs. *Spry1* not depicted as candidate target gene due to basemean<100 in MMe BMDMs.